Journal of Radioanalytical and Nuclear Chemistry (2022) 331:3535–3544
https://doi.org/10.1007/s10967-022-08416-9

Effect of soil properties on radioactivity concentrations and dose assessment

Amir M. González-Delgado[1] · **Punam Thakur**[1]

Received: 10 February 2022 / Accepted: 22 June 2022 / Published online: 19 July 2022

Abstract
This study evaluated the correlation between radioactivity concentrations and soil properties, and determined the total annual effective dose near an underground geologic repository for transuranic wastes. Soil samples were collected from two historical monitoring areas (Near Field and Cactus Flats). Alpha-particle spectrometry was used for the analysis of ^{241}Am, $^{239+240}$Pu and ^{238}U, while ^{137}Cs, ^{40}K, ^{232}Th and ^{226}Ra were detected by gamma ray spectrometry. Higher radioactivity concentrations and stronger positive correlations between radioactivity concentrations and soil properties were obtained in Cactus Flats compared to Near Field. The total annual effective dose was lower than the recommended limit of 1 mSv y^{-1}.

Keywords Actinides · Transuranic · Exposure pathways · Gamma · Dose rate

Introduction

Natural and anthropogenic radionuclides in soils have been reported to move to other environmental compartments through the food chain, leaching, soil resuspension and erosion processes [1–7]. The determination of radionuclides in the soil is required to evaluate the negative impacts of radioactive contamination on the environment and human health. Therefore, environmental monitoring of facilities responsible for the use of radioactive materials and management of radioactive wastes is relevant to ensure safe operations and evaluate radiological impacts on the environment and human health.

The Waste Isolation Pilot Plant (WIPP site) is located in southeastern New Mexico, USA and is an underground geologic repository for transuranic (TRU) wastes generated by the United States Department of Energy sites. In 2014, an accidental underground radiation release was caused by a runaway chemical reaction inside a TRU drum, a small portion of the contaminated air bypassed the ventilation filters and was discharged directly to the environment from an exhaust duct. The radiation release was reported to be below any level of public health or environmental concern [8]. Plutonium-239 + 240 ($^{239+240}$Pu) and americium-241 (^{241}Am) constitute more than 99% of the total radioactivity for disposal in the repository. Therefore, $^{239+240}$Pu and ^{241}Am are of interest for the environmental monitoring program of the WIPP site including uranium (^{238}U), potassium-40 (^{40}K), cesium-137 (^{137}Cs) and cobalt-60 (^{60}Co). Like ^{238}U and ^{40}K, radium-226 (^{226}Ra) and thorium-232 (^{232}Th) are known as naturally occurring radionuclides in the soil that contribute to terrestrial background radiation which is one of the main sources for radiation exposure of the World's population [9–11].

The land around the WIPP site is used for livestock grazing, potash mining, and oil/gas production. Workers conduct routine activities that could lead to exposure to radioactivity of the soil due to direct contact with the soil and suspension of fine soil particles during the operation of heavy equipment and strong wind events. Exposure to natural soil radiation takes place through external exposure to ionizing radiation, inhalation and ingestion of soil particles [12]. Also, workers could be exposed to anthropogenic radionuclides in the soil as result of global fallout caused by nuclear test sites and nuclear power plants accidents. Workers are potential human receptors for external exposure to ionizing radiation since they conduct regular outdoor activities across two soil monitoring areas (Near Field and Cactus

✉ Amir M. González-Delgado
agonzalez@cemrc.org

[1] Carlsbad Environmental Monitoring & Research Center, 1400 University Drive, 88220 Carlsbad, NM, USA

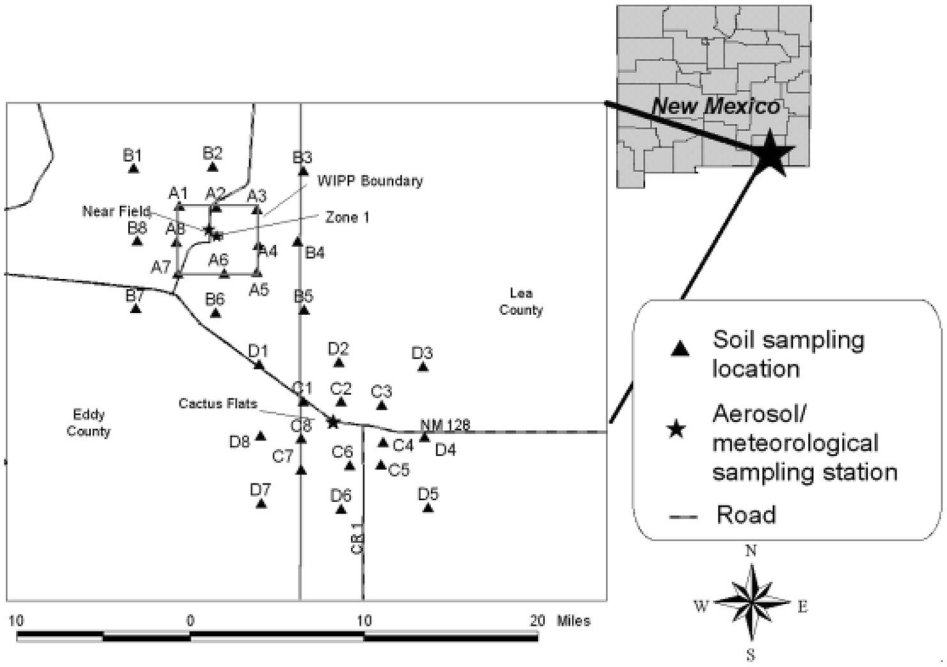

Fig. 1 Soil and aerosol sampling locations in the Waste Isolation Pilot Plant vicinity

Flats) located approximately 1 km northwest (downwind) and 19 km southeast (upwind) of the WIPP site. Previous studies reported external exposure to ionizing radiation as the exposure pathway with the highest cancer risk values [13, 14]. Therefore, the determination of potential damage to human health resulting from external exposure to ionizing radiation is necessary for the protection of workers.

The objectives of the study were to evaluate the relationship between radioactivity concentrations and soil properties, and determine the total annual effective dose (AED) for natural and artificial gamma emitting radionuclides detected in two soil monitoring areas located in the vicinity of the WIPP site. Information on the relationship between radionuclide concentrations and soil properties is relevant to understand the behavior of radionuclides in the environment and identify potential exposure pathways. Also the information generated in this study regarding the total AED as result of external exposure to ionizing radiation will be useful to evaluate the potential damage to human health in the vicinity of the WIPP site.

Materials and methods

Sample collection and analysis:

The study site has a non-calcareous, reddish sandy soil originated from eolian sand deposits over the Dewey lake red bed formation that mostly consist of reddish-brown siltstone and fine-grained sandstone The Dewey lake red bed is the uppermost formation in the Ochoan series followed by the Rustler, Salado (location of geologic repository for TRU wastes at approximately 655 m below the ground surface) and Castile formations [15]. A total of 64 (32 samples x 2 years) soil samples were collected from two locations (Site 107-Near Field and Site 108-Cactus Flats) where high-volume air samplers are located around the WIPP site in the Chihuahuan desert of southeastern New Mexico between 2015 and 2018 (Fig. 1). At both locations, a grid was established with sixteen undisturbed soil sampling locations.

Approximately 4 L of soil were collected using a trowel and a 50 × 50 cm frame with a depth of 0–2 cm and stored in plastic bags. All samples were air-dried for 24 h and passed through 2 mm sieve at the Carlsbad Environmental Monitoring and Research Center (CEMRC). A 50 g aliquot was used to determine the soil particle-size distribution using the pipette method described by Gee and Bauder [16]. The rest of the collected soil was oven dried at 105°C for 12 h then aliquots were used for soil organic matter (SOM), gamma and actinide analyses. Aliquots of 50 g of soil for each sample were used to determine the SOM content using the loss on ignition method [17]. Triplicates of 10 g of soil were placed in a muffle furnace at 500°C for 6 h.

Determination of gamma radionuclides in soil:

Aluminum paint cans of 300 g capacity were filled with soil, sealed and allowed radium nuclides (^{226}Ra and ^{228}Ra) to

reach equilibrium with daughter radionuclides for 25 days before conducting the gamma ray spectrometry analysis. Samples were counted for 48 h using high purity germanium detectors and spectral data was analyzed using Genie 2000 software (Mirion Technologies, Inc.). ^{232}Th activity was determined by using the energies of the progenies ^{228}Ac (338.3, 911.6 and 969.1 keV) and ^{212}Pb (238.6 keV). ^{226}Ra activity was measured by using the energies 295.2 and 351.9 keV of ^{214}Pb and 609.3, 1120.3, 1764.5 keV of ^{214}Bi. ^{137}Cs and ^{40}K activities were measured using the gamma energy lines 661.6 and 1460.8 keV, respectively.

Preparation of soil samples for determination of actinides:

Approximately 4-5 g of grounded soil was placed in the muffle furnace at 500°C for 6 h to eliminate the organic matter before conducting the radiochemical analysis for actinides [18]. Then, each sample was spiked with radioactive tracers (^{243}Am, ^{242}Pu and ^{232}U), sea sand was spiked with ^{241}Am, $^{239+240}$Pu and ^{238}U and used as laboratory control. Samples were digested in teflon beakers with 10 mL hydrochloric (HCL), 10 mL nitric (HNO_3), and 20 mL hydrofluoric (HF) acids on a hotplate at 200°C. The sample residues were heated with perchloric acid and boric acids to remove HF. Finally, the residues were dissolved in 8 M HNO_3 for radiochemical separation.

Separation of plutonium from americium and uranium:

The oxidation state of plutonium was adjusted to plutonium (IV) by adding 1 mL of 1 M ammonium iodide (NH_4I) with a 10 min wait step, followed by 1 mL of 2 M sodium nitrite ($NaNO_2$). Plutonium was separated from americium and uranium using an anion exchange resin (AG1-X8, 100–200 mesh, Cl^- form; Eichrom Technologies, Inc.) conditioned with 25 mL of 8 M HNO_3 [19]. Americium and uranium passed through the anion exchange resin column and the effluent was used for americium and uranium analysis. Thorium was removed from the column with 40 mL of 10 M HCL. Finally, plutonium was eluted with 30 mL of 0.1 M NH_4I + 10 M HCL solution that reduced the plutonium (IV) previously retained by the anion exchange resin column to plutonium (III).

The eluted plutonium fraction was evaporated with 3 mL of HNO_3 and 0.5 mL of 5 mg mL^{-1} iron carrier to complete dryness. The plutonium residue in the samples was dissolved in 4 mL of 2 M HCL, then 0.5 mL of 2 M $NaNO_2$ and 10 mL of HCL were added to complete the oxidation state adjustment of plutonium. The samples were passed through anion exchange resin columns previously conditioned with 25 mL of 8 M HCL to purify the plutonium fraction. The columns were washed with 30 mL of 8 M HCL before eluting plutonium with 30 mL of 0.1 M NH_4I + 8 M HCL. The collected plutonium samples were evaporated to complete dryness after adding 3 mL of HNO_3 and 0.5 mL of 5 mg mL^{-1} iron carrier.

Separation of americium and uranium:

The effluent solution containing the americium and uranium fractions was evaporated to dryness and dissolved in 10 mL of 2 M HNO_3. Uranium was separated from americium on TRU chromatography resin (tri n-butyl phosphate, N-diisobutyl carbamoxyl methyl phosphine oxide; Eichrom Technologies, Inc.) previously conditioned with 10 mL of 2 M HNO_3[19]. The presence of iron (III) in the samples interferes in the separation of americium (III) on the TRU column, therefore its presence was tested by adding 1 drop of ammonium thiocyanate (NH_4SCN) solution. Samples turned color red if the test was positive and approximately 10 drops of 1 M ascorbic acid solution were added until the red color disappeared indicating that iron (III) was reduced to iron (II). The samples were loaded into the TRU columns, washed with 10 mL of 2 M HNO_3 and washed a second time with 10 mL of 2 M HNO_3 + 0.05 M $NaNO_2$ to oxidize any plutonium (III) to plutonium (IV). Then americium (III) was eluted with 20 mL of 4 M HCL and uranium was eluted with 20 mL of 0.1 M ammonium bioxalate. After separation, the uranium fraction was evaporated to dryness with 5 mL of HNO_3 and 1 mL of 10% sodium sulfate (Na_2SO_4). Then the uranium samples were dissolved in 10 mL of 8 M HCL and purified by passing them through anion exchange resin columns previously conditioned with 25 mL of 8 M HCL. The columns were washed with 30 mL of 8 M HCL before eluting uranium with 30 mL of 1 M HCL. The uranium fraction was evaporated to dryness after adding 1 mL of 10% Na_2SO_4 and 5 mL of HNO_3.

The americium fraction collected from the TRU column was evaporated to dryness with 1 mL of 50% sulfuric acid and 3 mL of perchloric acid to destroy any TRU resin material present in the solution. The dried americium fraction was dissolved in 10 mL of 3 M NH_4SCN + 0.1 M formic acid (HCOOH). The solution was loaded onto a TEVA resin (Aliquot 336; Eichrom Technologies, Inc.) previously conditioned with 10 mL of 3 M NH_4SCN. The TEVA resin column was washed with 12 mL of 1.5 M NH_4SCN + 0.1 M HCOOH to remove lanthanides that could be present. Americium was eluted with 15 mL of 2 M HCL and the remaining NH_4SCN was destroyed by heating with 8–10 mL of HNO_3: HCL (1:3). Finally, the americium samples were evaporated to dryness. The dried americium, plutonium and uranium samples from the purification process

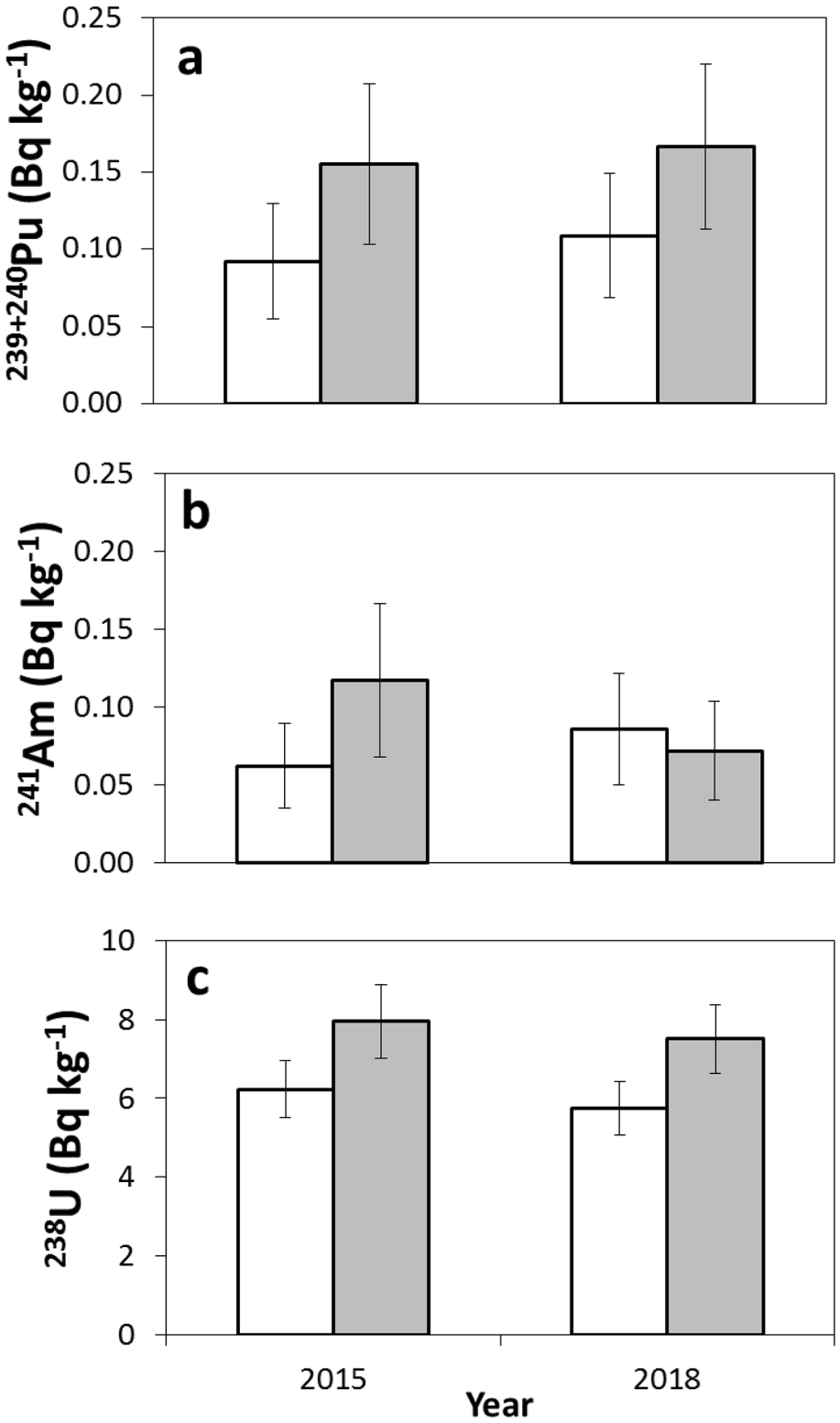

Fig. 2 Average plutonium-239 + 240 (a), americium-241 (b) and uranium-238 (c) activity concentrations in soil samples collected from Near Field (white columns) and Cactus Flats (grey columns) in 2015 and 2018. Error bars represent standard error

were dissolved with 4 mL of 2 M HCL and transferred to 50 mL polycarbonate centrifuge tubes with DI water. The samples were then micro-coprecipitated using 0.1 mL of 0.5 mg mL^{-1} neodymium-carrier and 1 mL of HF on stainless steel planchettes that were counted for five days using an APEX-Alpha spectrometer (Mirion Technologies, Inc.) [20].

Statistical analysis

Statistical significant difference of radionuclide concentrations, soil texture, pH and SOM in samples collected from both sites was determined using the t-test (SPSS software, IBM Corp, Armonk, NY, USA). Correlation analysis was used to evaluate the relationship between radionuclide concentrations and soil properties. Data collected in 2015 and 2018 were combined to conduct the correlation analysis.

Radiological characterization of ^{226}Ra, ^{232}Th^{40}K and ^{137}Cs:

The radiological characterization of ^{226}Ra, ^{232}Th ^{40}K and ^{137}Cs was conducted using the soil activity concentrations detected in 2018. Soil activity concentrations of ^{226}Ra, ^{232}Th, ^{40}K and ^{137}Cs were used to calculate the total absorbed gamma dose rate (D; nGy h^{-1}) in air at 1 m above the ground level using the conversion factors in Eq. (1):

$$D = 0.462A_{Ra} + 0.604A_{Th} + 0.0417A_{K} + 0.1125A_{Cs} \quad (1)$$

where A_{Ra}, A_{Th}, A_K and A_{Cs} are the activity concentrations (Bq kg^{-1}) of ^{226}Ra, ^{232}Th, ^{40}K and ^{137}Cs, respectively [9, 21–23].

The D values were converted to total annual effective doses using the method presented by UNSCEAR [9]. Total annual effective dose (AED; μSv y^{-1}) was calculated using Eq. (2) as:

$$AED = Dx8760x0.2x0.7x10^{-3} \quad (2)$$

where D (nGy h^{-1}) is total absorbed gamma dose rate in air at 1 m above the ground level, 8760 (h yr^{-1}) is the time conversion factor, 0.2 is the outdoor occupancy factor for a person spending 20% of time outdoors, 0.7 (Sv Gy^{-1}) is the conversion coefficient factor to convert outdoor gamma absorbed dose rate in air to effective dose received by adults and 10^{-3} is a conversion factor [9, 24].

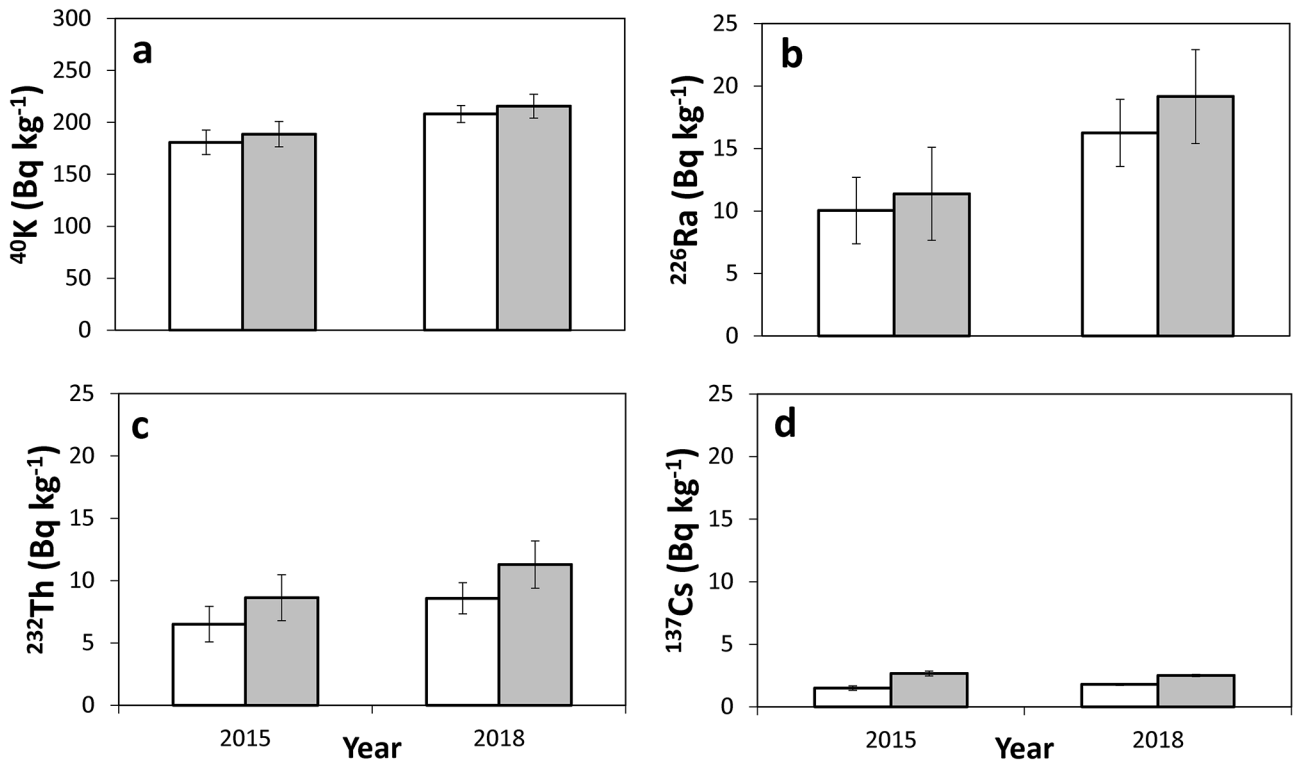

Fig. 3 Average potassium-40 (a), radium-226 (b), throrium-232 (c) and cesium-137 (d) concentrations in soil samples collected from Near Field (white columns) and Cactus Flats (grey columns) in 2015 and 2018. Error bars represent standard error

Results and discussion

Relationship between radioactivity concentrations and soil properties

^{241}Am, $^{239+240}$Pu, ^{238}U, ^{137}Cs, ^{40}K, ^{232}Th and ^{226}Ra were detected in soil samples collected from both locations, except for ^{60}Co. The radioactivity concentrations of ^{241}Am, $^{239+240}$Pu, and ^{137}Cs were representative of background levels due to global and regional (Nevada Test Site) fallout, and possibly soil resuspension from the Gnome site (underground nuclear test) located 8.8 Km southwest of the WIPP site [25, 26]. Radiological analysis of air filter samples collected from 1998 to 2010 showed that the exhaust air from the WIPP underground repository has not been a source of radiological contamination in the study site [27]. After the 2014 radiation release event at the WIPP site, ^{241}Am and $^{239+240}$Pu were reported to be the dominant radionuclides detected in air monitoring stations located within and outside the WIPP [8]. Detected ^{241}Am and $^{239+240}$Pu concentrations in air filters were low and no adverse health effects on WIPP workers were observed after the 2014 radiation release event [28]. Thakur [29] reported that $^{239+240}$Pu and ^{241}Am concentrations in air filter samples reached pre-release levels two weeks later after the 2014 radiation release event. This confirms that $^{239+240}$Pu and ^{241}Am concentrations detected in ambient air filter samples were originated due to the resuspension of soil particles contaminated by nuclear weapon fallout.

Most of the soil radionuclide concentrations were significantly higher in Cactus Flats than in Near Field ($p < 0.05$), except for ^{40}K and ^{226}Ra concentrations that were similar at both locations while ^{241}Am concentrations were not significantly different in 2018 (Figs. 2 and 3). Differences of concentrations in both locations could be explained by differences in soil properties. The soils in Near Filed and Cactus Flats were well-drained, non-calcareous with a carbonate content < 1% and developed from eolian sand parent materials [30, 31]. Both locations had a sand texture classification, however silt, clay and SOM contents were significantly greater in Cactus Flats than in Near Field, while the sand content was greater in Near Field ($p < 0.05$) (Table 1).

Sand showed a negative correlation with silt (r = -0.80, $p < 0.01$), clay (r = -0.88, $p < 0.01$), SOM (r = -0.25, $p = 0.17$) and pH (r = -0.40, $p < 0.05$) in Near Field. While similar relationships were obtained for sand with silt (r = -0.75, $p < 0.01$), clay (r = -0.71, $p < 0.01$), SOM (r = -0.58, < 0.01) and pH (r = -0.14, $p = 0.47$) in Cactus Flats. Clay content was positively correlated with SOM in Cactus Flats ($r = 0.46$, $p < 0.05$), however the correlation was not significant in Near Field ($r = 0.24$, $p = 0.19$). Silt and clay contents were positively correlated in Near Field (0.67, $p < 0.01$) and Cactus Flats (0.46, $p < 0.05$). Fine soil particles (clay and silt) are able to interact with radionuclides through the adsorption process for having greater surface area compared to sand particles. Clay is the finest of the soil particles, therefore it has more surface area available for sorption sites for

Table 1 Average soil properties of samples collected from Near Field and Cactus Flats

	Near Field	Cactus Flats
Sand (%)†	94.9 ± 1.9	91.8 ± 3.2
Silt (%)†	2 ± 0.9	3.6 ± 1.8
Clay (%)†	3.1 ± 1	4.5 ± 1.5
SOM (%)*	1 ± 0.2	1.1 ± 0.3
pH†	7.3 ± 0.5	7.5 ± 0.4

†Average ± standard deviation values from measurements conducted in 2015

*SOM; soil organic matter, average ± standard deviation values from measurements conducted in 2015 and 2018

Table 2 Correlation between radioactivity concentrations and soil properties

Location	Analyte	Sand %	Silt %	Clay %	OM %	pH
Near Field	$^{239+240}$Pu	0.14	-0.17	-0.08	0.50**	-0.09
	^{241}Am	-0.23	0.19	0.31	0.45**	0.35*
	^{238}U	-0.02	-0.02	0.08	0.30**	0.13
	^{40}K	-0.19	0.10	0.27**	0.44**	0.07
	^{137}Cs	-0.06	-0.01	0.13	0.24	0.18
	^{232}Th	-0.17	0.11	0.24	0.26	0.13
	^{226}Ra	-0.12	0.08	0.17	0.14	0.05
Cactus Flats	$^{239+240}$Pu	-0.11	0.21	-0.02	0.25*	-0.03
	^{241}Am	-0.21	0.20	0.12	0.08	0.05
	^{238}U	-0.47**	0.40**	0.43**	0.38**	0.22
	^{40}K	-0.51**	0.48**	0.47**	0.76**	0.21
	^{137}Cs	-0.30*	0.33**	0.21	0.45**	0.01
	^{232}Th	-0.44**	0.36**	0.38**	0.70**	0.1
	^{226}Ra	-0.30**	0.23	0.31**	0.58**	0.09

Correlations significant (**) and (*) at the 0.01 and 0.05 levels, respectively

Table 3 Radioactivity concentrations of gamma-emitting radionuclides and their radiological risk characterization parameters for soil samples from Near Field (Grid A-B) and Cactus Flats (Grid C-D)

Grid	^{226}Ra (Bq kg^{-1})	^{232}Th (Bq kg^{-1})	^{40}K (Bq kg^{-1})	^{137}Cs (Bq kg^{-1})	D (nGy h^{-1})	AEDE (μSv y^{-1})
A-1	17.1 ± 1.5	7.9 ± 0.74	181.2 ± 7.3	0.9 ± 0.1	20.4	24.9
A-2	17.9 ± 1.7	9.3 ± 1.2	215.4 ± 8.5	2.3 ± 0.1	23.1	28.4
A-3	12.3 ± 1.2	6.7 ± 0.6	172.6 ± 6.9	1.4 ± 0.1	17.1	20.9
A-4	17.3 ± 1.6	9.4 ± 1.3	206.2 ± 8.2	1.8 ± 0.1	22.5	27.6
A-5	13 ± 0.5	6.8 ± 0.6	187.9 ± 7.5	1.2 ± 0.1	18.1	22.2
A-6	16.1 ± 1.6	9 ± 1.1	234.3 ± 9.3	1.3 ± 0.1	22.8	27.9
A-7	17.8 ± 1	8.7 ± 0.8	224.4 ± 8.9	2.9 ± 0.1	23.2	28.4
A-8	18.5 ± 1.4	9.4 ± 0.9	232.5 ± 9.3	1.2 ± 0.1	24.1	29.5
B-1	21. ± 1	10.5 ± 1.4	261.9 ± 10.3	2.9 ± 0.1	27.3	33.5
B-2	16.7 ± 1.1	8.8 ± 0.8	212.2 ± 8.5	1 ± 0.1	22	27
B-3	20.9 ± 2.1	11.3 ± 1.0	264.2 ± 11	4.2 ± 0.1	27.9	34.3
B-4	14.8 ± 0.5	8.9 ± 1.2	195.3 ± 7.8	1.5 ± 0.1	20.6	25.2
B-5	13.6 ± 1.8	7.1 ± 0.6	163.5 ± 6.6	1.6 ± 0.1	17.6	21.5
B-6	12.5 ± 0.3	7.1 ± 0.9	183.9 ± 7.3	1.1 ± 0.1	17.9	21.9
B-7	16.9 ± 1.6	8.2 ± 0.8	188.2 ± 7.5	1.9 ± 0.1	20.8	25.5
B-8	13.3 ± 0.3	8.3 ± 1.1	205.4 ± 8.1	1.6 ± 0.1	19.9	24.4
C-1	20.5 ± 2.1	14.4 ± 1.3	256.8 ± 10.2	2.7 ± 0.1	29.2	35.8
C-2	13.4 ± 0.2	8.4 ± 1.1	131.8 ± 5.3	1 ± 0.1	16.9	20.7
C-3	25.2 ± 1.7	13.4 ± 1.2	240.6 ± 9.6	3.6 ± 0.1	30.1	36.9
C-4	18.3 ± 0.6	10.7 ± 1.5	206 ± 8.2	3.4 ± 0.1	23.9	29.3
C-5	16.2 ± 1.5	9.2 ± 0.8	177.7 ± 7.1	2.7 ± 0.1	20.7	25.4
C-6	21.1 ± 3.5	11.9 ± 2.3	217.8 ± 19.8	2.7 ± 0.1	26.3	32.3
C-7	24 ± 1	13.5 ± 1.6	268.6 ± 10.7	4.2 ± 0.1	30.9	37.9
C-8	25.8 ± 4.1	14.4 ± 2.3	280.2 ± 25.5	2.7 ± 0.1	32.6	39.9
D-1	18.4 ± 1.7	9.8 ± 1.2	208.5 ± 8.3	2.6 ± 0.1	23.4	28.7
D-2	17.4 ± 0.7	9.9 ± 0.9	181.6 ± 7.3	2.7 ± 0.1	21.9	26.8
D-3	16.2 ± 2.6	9.5 ± 1.4	199.5 ± 18.2	1.9 ± 0.1	21.7	26.7
D-4	17.5 ± 1.7	12.3 ± 1.5	208 ± 8.3	2.8 ± 0.1	24.5	30
D-5	21.1 ± 1	11.5 ± 1.0	208.6 ± 8.4	2.1 ± 0.1	25.6	31.4
D-6	20.7 ± 1.9	12 ± 1.4	236 ± 9.3	3.2 ± 0.1	27	33.2
D-7	11.9 ± 1.3	8.7 ± 1.1	205.6 ± 8.2	0.7 ± 0.1	19.4	23.8
D-8	18.9 ± 3.3	11.3 ± 1.8	221.6 ± 20.2	1.2 ± 0.1	24.9	30.6

D; total adsorbed gamma dose rate, AED; total annual effective dose. Average ± Standard deviation values for radioactivity concentrations of ^{226}Ra, ^{232}Th ^{40}K and ^{137}Cs

solutes [32, 33]. Studies have reported that soils with high clay content have better capacity to preserve organic matter than those having low clay content [34, 35].

Kirchner [25] reported strong correlations between radionuclide concentrations and soil texture, but the relationship between radionuclide concentrations and SOM was not examined for soil samples collected from Near Field and Cactus Flats in 1998. Similarly, Thakur [26] reported that $^{239+240}$Pu concentration was positively correlated with the aerosol mass retained in ambient air filters from air monitoring stations located at the WIPP site, Near Field and Cactus Flats during 1998–2010. Also $^{239+240}$Pu and ^{137}Cs concentrations showed a decreasing trend with increasing soil depth in the WIPP vicinity. $^{239+240}$Pu, ^{241}Am and ^{137}Cs concentrations in soil samples collected from Near Field after the 2014 radiation release event were not adverse to human health, however, radionuclide concentrations in soil samples from the Cactus Flats location and the influence of soil properties on radionuclide concentrations were not evaluated [28].

$^{239+240}$Pu, ^{238}U, ^{40}K, showed a positive correlation with SOM at both locations (Table 2). ^{241}Am concentration was positively correlated with SOM, while ^{40}K concentration also showed a positive correlation with silt content, however there was no significant correlation between soil properties and the rest of radionuclides (^{137}Cs, ^{232}Th and ^{226}Ra) in Near Field. In contrast, ^{238}U, ^{40}K and ^{137}Cs, ^{232}Th and ^{226}Ra were negatively correlated with sand content and

positively correlated with SOM in Cactus Flats. Also most of the radionuclides were significantly correlated with silt and clay contents in Cactus Flats. Previous studies reported that concentrations of natural gamma-emitting radionuclide (^{232}Th, ^{40}K, and ^{226}Ra) and ^{137}Cs were positively correlated with clay and SOM [33, 36, 37]. Also ^{241}Am, $^{239+240}$Pu, ^{238}U have shown greater affinity for finer soil particles and SOM during laboratory and field studies that used soils from different climate regions [25, 38–45].

Generally, there was no significant relationship between pH and radionuclide concentrations. The lack of correlation between pH and radionuclide concentrations could be due to the narrow range of soil pH values [46]. Previous studies have reported weak or no correlations between pH and radionuclide concentrations in different soil types [26, 47–49]. In contrast, other studies reported a negative correlation between pH and radionuclide concentrations [37, 50, 51].

Radiological characterization of detected gamma emitting radionuclides

Average ^{226}Ra, ^{232}Th, ^{40}K and ^{137}Cs concentrations in Near Field were 16.3 ± 2.7, 8.6 ± 1.2, 208 ± 29 and 1.8 ± 0.9, respectively, while ^{226}Ra, ^{232}Th, ^{40}K and ^{137}Cs concentrations in Cactus Flats were 19.2 ± 4, 11.3 ± 2, 216 ± 35 and 2.5 ± 0.9, respectively (Table 3). Concentrations at both sites were lower than the worldwide average values for ^{226}Ra (35 Bq kg^{-1}), ^{232}Th (30 Bq kg^{-1}), ^{40}K (400 Bq kg^{-1}) and ^{137}Cs (51 Bq kg^{-1}) [9, 11, 23, 52]. ^{40}K was the major contributor to the calculated D and AED followed by ^{226}Ra > ^{232}Th > ^{137}Cs. Similarly, Hannan [22] reported that even with the additional contribution of ^{137}Cs the D and AED values were lower than the global average D (59 nGy h^{-1}) and AED (70 µSv y^{-1}) values calculated based on the contribution from natural gamma-emitting radionuclides. The average D values of 21.6 ± 3.1 nGy h^{-1} for Near Field and 24.9 ± 4.2 nGy h^{-1} for Cactus Flats were significantly different ($p < 0.05$). All of the AED values estimated for each of the grid nodes were less than 1mSv y^{-1}, with average AED values of 26.5 ± 3.8 and 30.6 ± 5.2 µSv y^{-1} for Near Field and Cactus Flats, respectively (Table 4). The estimated AED values were relatively similar compared to a study conducted in Qatar (27 µSv y^{-1}), but lower than AED values from Texas-USA (59 µSv y^{-1}), Taiwan (60.5 µSv y^{-1}), Nigeria (70 µSv y^{-1}); and Malaysia (169 µSv y^{-1}) [10, 11, 22, 33, 50].

Conclusions

The Cactus Flats location had higher soil radioactivity concentrations, SOM and percentage of fine soil particles

Table 4 Comparison of radioactivity concentrations of gamma-emitting radionuclides and their radiological risk characterization parameters for soil samples collected from different countries of the world

Location	^{226}Ra (Bq kg^{-1})	^{232}Th (Bq kg^{-1})	^{40}K (Bq kg^{-1})	^{137}Cs (Bq kg^{-1})	D (nGy h^{-1})	AEDE (µSv y^{-1})	Reference
Near Field	16.3	8.6	208	1.8	21	26	Present work
Cactus Flats	19.2	11.3	216	2.5	24	30	Present work
Qatar	17	10	201	4	22	27	[33]
USA	33.7	-----	299.7	3.7	48	59	[22]
Turkey	-----	51.8	344.9	26.3	56	69	[23]
Nigeria	41	29.7	412.5	-----	55	68	[10]
Malaysia	102.1	133.9	325.9	-----	141	169	[11]

D; total adsorbed gamma dose rate, AED; total annual effective dose. Radioactivity concentrations of ^{226}Ra, ^{232}Th ^{40}K and ^{137}Cs

compared to the Near Field location. Therefore, stronger relationships between soil radioactivity concentrations and soil properties were obtained in Cactus Flats. Soil radioactivity concentrations showed a positive correlation with silt, clay, and SOM, however they were negatively correlated with sand content and either not or weakly correlated with soil pH. The AED values were lower than the recommended limit, meaning that soil radioactivity concentrations from detected natural and artificial gamma-emitting radionuclides in the soil around the WIPP site are safe to human health.

Acknowledgements This research is supported by the U.S. Department of Energy, Carlsbad Field Office through grant No. DE-EM 0005159. The opinions, findings, and conclusions expressed are those of the authors and do not necessarily reflect the views of the sponsors. Authors thank Savannah Hixon and Jim Monks from CEMRC for providing the soil samples.

Declarations

Competing interests The authors have no competing interests to declare that are relevant to the content of this article.

References

1. Al-Oudat M, Asfary AF, Mukhalallti H, Al-Hamwi A, Kanakri S (2006) Transfer factors of ^{137}Cs and ^{90}Sr from soil to trees in arid regions. J Environ Radioact 90(1):78–88
2. Lujaniene G, Valiulis D, Bycenkiene S, Sakalys J, Povinec PP (2012) Plutonium isotopes and ^{241}Am in the atmosphere of Lithuania: A comparison of different source terms. Atmos Environ 61:419–427
3. Lokas E, Bartmiński P, Wachniew P, Mietelski JW, Kawiak T, Środoń J (2014) Sources and pathways of artificial radionuclides to soils at a High Arctic site. Environ Sci Pollut Res 21(21):12479–12493
4. Zheng MJ, Murad A, Zhou XD, Yi P, Alshamsi D, Hussein S, Chen L, Hou XL, Aldahan A, Yu ZB (2016) Distribution and sources of ^{226}Ra in groundwater of arid region. J Radioanal Nucl Chem 309:667–675
5. Alewell C, Pitois A, Meusburger K, Ketterer M, Mabit L (2017) $^{239+240}$Pu from "contaminant" to soil erosion tracer: Where do we stand? Earth Sci Rev 172:107–123
6. Madzunya D, Dudu VP, Mathuthu M, Manjoro M (2020) Radiological health risk assessment of drinking water and soil dust from Gauteng and North West Provinces, in South Africa. Heliyon 6(2):e03392. https://doi.org/10.1016/j.heliyon.2020.e03392
7. Bulubasa G, Costinel D, Miu AF, Ene MR (2021) Activity concentrations of ^{238}U, ^{232}Th, ^{226}Ra ^{137}Cs and ^{40}K radionuclides in honey samples from Romania. Lifetime cancer risk estimated. J Environ Radioact 234:106626. DOI: https://doi.org/10.1016/j.jenvrad.2021.106626
8. Thakur P (2016) Source term estimation and the isotopic ratio of radioactive material released from the WIPP repository in New Mexico, USA. J Environ Radioact 151:193–203
9. United Nations Scientific Committee on the Effects of Atomic Radiation (UNSCEAR) (2000) Sources and effects of ionizing radiation. New York
10. Agbalagba EO, Avwiri GO, Chad-Umoreh YE (2012) ɣ-Spectroscopy measurement of natural radioactivity and assessment of radiation hazard indices in soil samples from oil fields environment of Delta State, Nigeria. J Environ Radioact 109:64–70
11. Alzubaidi G, Hamid FBS, Rahman IA (2016) Assessment of natural radioactivity levels and radiation hazards in agricultural and virgin soil in the state of kedah, North of Malaysia. Sci World J. https://doi.org/10.1155/2016/6178103
12. Abdelbary HM, Elsofany EA, Mohamed YT, Abo-Aly MM, Attallah MF (2019) Characterization and radiological impacts assessment of scale TENORM waste produced from oil and natural gas production in Egypt. Environ Sci Pollut Res 26:30836–30846
13. Ziajahromi S, Khanizadeh M, Nejadkoorki F (2015) Using the RESRAD code to assess human exposure risk to ^{226}Ra, ^{232}Th, and ^{40}K in soil. Hum Ecol Risk Assess 21(1):250–264
14. Towle KM, Jacobs NFB, Keenan JJ, Monnot AD (2018) The cancer risk associated with residential exposure to soil containing radioactive coal combustion residuals. Risk Anal 38(6):1107–1115
15. Bachman GO (1984) Regional geology of ochoan evaporates, northern part of Delaware basin. New Mexico State Records Center and Archives, p 184
16. Gee GW, Bauder JW(1986) Particle size analysis. A. Klute (ed.). Methods of Soil Analysis, Part I, Physical and Mineralogical Methods, 2nd Edition, 9(1):383–411, American Society of Agronomy, Madison, WI
17. Nelson DW, Sommers LE(1996) Total Carbon, Organic Carbon, and Organic Matter. In Methods of Soil Analysis, Part 3. Chemical Methods, 961–1009. Soil Science Society of America. Madison WI
18. Carlsbad Environmental Monitoring & Research Center (CEMRC) (2010) Report. Carlsbad, New Mexico
19. Thakur P, Ballard S, Conca JL (2011) Sequential isotopic determination of plutonium, thorium, americium and uranium in the air filter and drinking water samples around the WIPP site. J Radioanal Nucl Chem 287:311–321
20. Hindman FD (1983) Neodymium fluoride mounting for alpha spectrometric determination of uranium, plutonium and americium. Anal Chem 55:2460–2461
21. United Nations Scientific Committee on the Effects of Atomic Radiation (UNSCEAR) (2008) Sources and effects of ionizing radiation. New York
22. Hannan M, Wahid K, Nguyen N (2015) Assessment of natural and artificial radionuclides in Mission (Texas) surface soils. J Radioanal Nucl Chem 305(2):573–582
23. Durusoy A, Yildirim M (2017) Determination of radioactivity concentrations in soil samples and dose assessment for Rize Province, Turkey. J Radiat Res Appl Sc 10(4):348–352
24. United Nations Scientific Committee on the Effects of Atomic Radiation (UNSCEAR) (1988) Sources, effects and risk of ionizing radiation. New York
25. Kirchner TB, Webb JL, Webb SB, Arimoto R, Schoep DA, Stewart BD (2002) Variability in background levels of surface soil radionuclides in the vicinity of the US DOE waste isolation pilot plant. J Environ Radioact 60(3):275–291
26. Thakur P, Ballard S, Nelson R (2012) Plutonium in the WIPP environment: its detection, distribution and behavior. J Environ Monit 14:1604–1615
27. Thakur P, Mulholland GP (2011) Monitoring of gross alpha, gross beta and actinides activities in exhaust air released from the waste isolation pilot plant. Appl Radiat Isot 69:1307–1312
28. Thakur P, Lemons BG, Ballard S, Hardy R (2015) Environmental and health impacts of February 14, 2014 radiation release from the nation's only deep geologic nuclear waste repository. J Environ Radioact 146:6–15
29. Thakur P, Lemons BG, White CR (2016) The magnitude and relevance of the February 2014 radiation release from the Waste

Isolation Pilot Plant repository in New Mexico, USA. Sci Total Environ 565:1124–1137
30. Chugg JC, Anderson GW, King DL, Jones LH (1971) Soil survey of eddy county, New Mexico. United States Department of Agriculture, Washington, DC
31. Turner MT, Cox DN, Mickelson BC, Roath AJ, Wilson CD (1974) Soil survey of lea county, New Mexico. United States Department of Agriculture, Washington, DC
32. Oorts K, Vanlauwe B, Merckx R (2003) Cation exchange capacities of soil organic matter fractions in a ferric lixisol with different organic matter inputs. Agric Ecosyst Environ 100(2):161–171
33. Ahmad AY, Al-Ghouti MA, AlSadig I, Abu-Dieyeh M (2019) Vertical distribution and radiological risk assessment of ^{137}Cs and natural radionuclides in soil samples. Sci Rep 9:12196. https://doi.org/10.1038/s41598-019-48500-x
34. Vanden Bygaart AJ, Kay BD (2004) Persistence of soil organic carbon after plowing a long-term no-till field in southern Ontario, Canada. Soil Sci Soc Am J 68(4):1394–1402
35. Azlan A, Aweng ER, Ibrahim CO, Noorhaidah A (2012) Correlation between soil organic matter, total organic matter and water content with climate and depths of soil at different land use in Kelantan, Malaysia. J Appl Sci Environ Manag 16(4):346–358
36. Al-Sulaiti H, Nasir T, Regan PH, Bradley D, Al-Mugren K, Alkhomashi N, Al-Dahan N, Al-Dosari M, Bukhari SJ, Matthews M, Santawamaitre T, Malain D, Habib A (2014) Effect of the grain size of the soil on the measured activity and variation in activity in surface and sub surface soil samples. Pak j sci ind res Ser A: phys sci 57(3):129–138
37. Mesrar H, Sadiki A, Faleh A, Quijano L, Gaspar L, Navas A (2017) Vertical and lateral distribution of fallout ^{137}Cs and soil properties along representative toposequences of central Rif, Morocco. J Environ Radioact 169–170:27–39
38. Vyas BN, Mistry KB (1981) Influence of clay mineral type and organic matter content on the uptake of ^{239}Pu and ^{241}Am in by plants. Plant and Soil 59(1):75–82
39. Lee MH, Lee CW (2000) Association of fallout-derived ^{137}Cs, ^{90}Sr and ^{239,240}Pu with natural organic substances in soils. J Environ Radioact 47(3):253–262
40. Sokolik G, Ovsiannikova S, Kimlenko I (2002) Soil organic matter and migration properties of $^{239–240}$Pu and ^{241}Am. Radioprotection – Colloques 37:283–288
41. Ovsiannikova S, Papenia M, Voinikava K, Brown J, Skipperud L, Sokolik G, Svirschevsky S (2010) Migration ability of plutonium and americium in the soils of Polessie State Radiation-Ecological Reserve. J Radioanal Nucl Chem 286:409–415
42. Wasserman MAV, Pereira TR, Rochedo ERR, Sousa WO, Pérez DV, Pinheiro EFM, Simões Filho FFL (2011) The influence of Brazilian soils properties in Americium sorption. Radioprotection 46(6):S579–S585
43. Kumar A, Rout S, Mishra MK, Karpe R, Ravi PM, Tripathi RM (2015) Impact of particle size, temperature and humic acid on sorption of uranium in agricultural soils of Punjab. SpringerPlus 4:262
44. Xu C, Zhang S, Sugiyama Y, Ohte N, Ho YF, Fujitake N, Kaplan DI, Yeager CM, Schwehr K, Santschi PH (2016) Role of natural organic matter on iodine and ^{239,240}Pu distribution and mobility in environmental samples from the northwestern Fukushima Prefecture, Japan. J Environ Radioact 153:156–166
45. Yang S, Zhang X, Wu X, Li M, Zhang L, Huang Q (2019) Adsorption characteristics of U (VI) in the soil horizons near uranium tailing impoundment area. Int J Eng Technol 11(1):44–47
46. Morton LS, Evans CV, Estes GO (2002) Natural uranium and thorium distributions in podzolized soils and native blueberry. J Environ Qual 31(1):155–162
47. Navas A, Soto J, Machín J (2002) Edaphic and physiographic factors affecting the distribution of natural gamma-emitting radionuclides in the soils of the Arnás catchment in the Central Spanish Pyrenees. Eur J Soil Sci 53(4):629–638
48. Vukašinović I, Đorđević A, Rajković MB, Todorović D, Pavlović VB (2010) Distribution of natural radionuclides in anthrosol-type soil. Turk J Agric For 34(6):539–546
49. Okedeyi AS, Gbadebo AM, Mustapha AO (2014) Effects of physical and chemical properties on natural radionuclides level in soil of quarry sites in Ogun State, Nigeria. J Appl Sci 14(7):691–696
50. Tsai TL, Liu CC, Chuang CY, Wei HJ, Men LC (2011) The effects of physico-chemical properties on natural radioactivity levels, associated dose rate and evaluation of radiation hazard in the soil of Taiwan using statistical analysis. J Radioanal Nucl Chem 288(3):927–936
51. Hegazy AK, Afifi SY, Alatar AA, Alwathnani HA, Emam MH (2013) Soil characteristics influence the radionuclide uptake of different plant species. Chem Ecol 29(3):255–269
52. Zubair M, Shafiqullah (2020) Measurement of natural radioactivity in several sandy-loamy soil samples from Sijua. Dhanbad India Heliyon 6(3):e03430. DOI:https://doi.org/10.1016/j.heliyon.2020.e03430